Low-Complex Frame Synchronization in OFDM Systems

Jan-Jaap van de Beek* Magnus Sandell* Mikael Isaksson† Per Ola Börjesson*

* Div. of Signal Processing
Luleå University of Technology
S–971 87 Luleå, Sweden

† Telia Research AB
S–977 75 Luleå, Sweden

Abstract – In this paper a novel data-based frame synchronization method for OFDM-systems is presented. OFDM frames are shown to contain sufficient information to synchronize a system without the use of pilots. The cyclic extension, preceding OFDM frames, is of decisive importance for this method. Based on only the sign bits of the in-phase and the quadrature components of the received OFDM signal, the maximum likelihood solution is derived. This solution basically consists of a correlator, a moving sum and a peak detector. The stability of the generated frame-clock is improved significantly by averaging over a few number of frames. Simulations show that this low-complex, averaging method can be used to synchronize an OFDM system on twisted pair copper wires and in slowly fading radio channels.

I. Introduction

Orthogonal frequency-division multiplexing (OFDM) systems have gained an increased interest during the last years [1]. Their use in wireless applications such as digital broadcast radio [2] and television [3], as well as mobile communication systems [4], is currently investigated.

By the name of *discrete multitone* (DMT) modulation, OFDM is also examined for broadband digital communication on the existing copper network. The OFDM technique has been proposed both for *high bit-rate digital subscriber lines* (HDSL) and *asymmetric digital subscriber lines* (ADSL) [5, 6].

A problem in the design of OFDM receivers and receivers for block transmission systems in general, is the unknown time instant to start sampling a new frame. Such a frame clock may be generated with the aid of pilot symbols known to the receiver [7]. The structure of the transmitted OFDM signal, however, offers the opportunity to generate a frame clock that works without the aid of such pilots.

In this paper we present and evaluate a novel method of synchronizing frames in OFDM systems. Two key elements will rule the entire discussion. The first element is the idea that the data itself contains sufficient information to perform satisfactory synchronization. This concept is also discussed in [8], and, for the estimation of a frequency offset, in [9]. The frame synchronization methods we present exploit the cyclic extension preceding the symbol frames, commonly accepted as a means to mitigate *inter-symbol interference* (ISI) in OFDM systems [1, 2]. The use of pilots is thus avoided. The second element is the demand that the methods must be low-complex and hence attractive to implement. We present methods, that only use the in-phase and quadrature sign bits of the OFDM data.

In Section II, the OFDM transmission model is described. The synchronization problem is formulated, and optimal solutions are presented in Section III. Finally, in Section IV, simulation results are given for transmission over typical copper wire channels and slowly fading radio channels.

II. The OFDM Model

Consider the transmission of complex numbers x_k, taken from some signal constellation (e.g., PSK, QAM). Fig. 1 illustrates the discrete-time OFDM system model we will use in the sequel. The data x_k are modulated on N subcarriers by an *inverse discrete Fourier transform* (IDFT) and the last L samples are copied and put as a preamble (cyclic prefix) to form the OFDM frame s_k.

The channel impulse response $h(k)$ is, for now, assumed to affect the signal $s(k)$ only by complex, additive white Gaussian noise (AWGN), $n(k)$, *i.e.*, $h(k) = \delta(k)$. In Section IV we consider other channel impulse responses. Thus, the received signal, $r(k)$, is given by

$$r(k) = s(k) + n(k). \tag{1}$$

The data y_k are obtained by discarding the first L samples (cyclic prefix) of $r(k)$ and demodulating the N remaining samples of each frame by means of a DFT.

The structure of the transmitted signal $s(k)$ is illustrated in Fig. 2. We assume that the data x_k constitute a white process. Further, if the number of subcarriers is sufficiently large, then $s(k)$ is approximately a complex Gaussian process, whose real and imaginary parts are independent [10]. This process, however, is not white, since the appearance of a cyclic extension yields a non-zero correlation between pairs of samples, part of the cyclic extension, spaced N samples apart. Thus, $r(k)$ is not a white process either. On the contrary, $r(k)$ contains information about when a new frame starts by its probabilistic

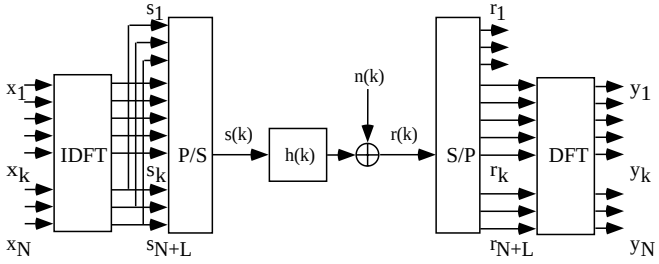

Fig. 1: OFDM system.

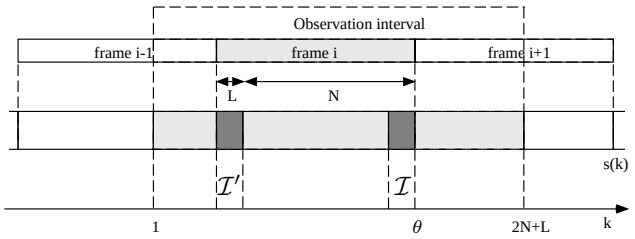

Fig. 2: Structure of OFDM signal with cyclicly extended frames, $s(k)$.

structure. This is the crucial observation that offers the opportunity for frame synchronization based on $r(k)$. In the next section, this idea is formally shaped and elaborated.

III. Synchronization Methods

A. Optimal Synchronization

Assume that we observe $2N+L$ consecutive samples of $r(k)$, *cf.* Fig. 2, and that these samples contain one complete $(N+L)$-sample OFDM frame. Notice that the other N samples in this observation interval are independent.

The position of this frame within the observed block of samples, however, is unknown. Define the integer time instant θ as the time index of the last sample of this frame, and the index sets $\mathcal{I} \triangleq [\theta-L+1, \theta]$ and $\mathcal{I}' \triangleq [\theta-N-L+1, \theta-N]$, see Fig. 2. The set $\mathcal{I}$ thus contains the indices of the data samples that are copied into the cyclic prefix, and the set $\mathcal{I}'$ contains the indices of this prefix.

In [11] it is shown that the log-likelihood function for the time instant θ given the observations $r(k), k = 1, \ldots, 2N+L$ is

$$\Lambda_{\mathrm{r}}(\theta) = \tag{2}$$
$$= \sum_{k=\theta-L+1}^{\theta} 2(1-\rho)\mathrm{Re}\{r(k)r^*(k-N)\} - \rho \cdot |r(k)-r(k-N)|^2$$

where

$$\rho = \frac{E\{|s(k)|^2\}}{E\{|s(k)|^2\}+E\{|n(k)|^2\}} = \frac{\mathrm{SNR}}{\mathrm{SNR}+1} \tag{3}$$

is the correlation coefficient of a sample $r(k), k \in \mathcal{I}$ and the sample $r(k-N)$ in the cyclic prefix. The signal-to-noise ratio (SNR) is defined as $E\{|s(k)|^2\}/E\{|n(k)|^2\}$.

The *maximum likelihood* (ML) estimation of θ given $r(k)$, $\hat{\theta}_r$, is the argument maximizing (2). Thus, depending on SNR, the correlation and the squared difference between received data samples spaced N samples apart are weighted in an optimal way, the correlation term positively and the squared difference term negatively. This estimate, $\hat{\theta}_r$, whose implementation may be complex, will be used as a reference in Section IV.

B. Low-Complex Synchronization

In the discussion that follows, we will comply with the objective that the synchronization must be low-complex, and we quantize the in-phase and quadrature components of $r(k)$ to form the complex sequence $c(k) = Q[r(k)], k = 1, \ldots, 2N+L$ where $Q[\cdot]$ denotes the complex quantizer

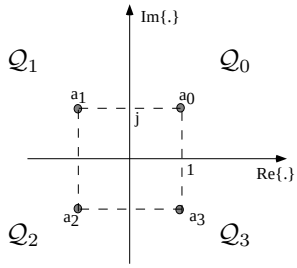

Fig. 3: Geometric representation of the signal set $\mathcal{A}$ and the quadrants $\mathcal{Q}_i, i = 0, 1, 2, 3$ of the complex plane.

$$Q[x] \triangleq \mathrm{sign}\left(\mathrm{Re}\{x\}\right) + j\,\mathrm{sign}\left(\mathrm{Im}\{x\}\right), \tag{4}$$

$$\mathrm{sign}(x) \triangleq \begin{cases} +1, & x \geq 0, \\ -1, & x < 0. \end{cases} \tag{5}$$

The signal $c(k)$ is a complex bitstream, *i.e.*, $c(k)$ can only take one of four different values in the alphabet

$$\mathcal{A} = \{a_0, a_1, a_2, a_3\}, \ \{1+j, -1+j, -1-j, 1-j\}, \tag{6}$$

see Fig. 3. The sequence $c(k)$ can thus be represented by 2 bits, one for its real and one for its imaginary part. In spite of this quantization, $c(k)$ still contains information about θ. A sample $c(k), k \in \mathcal{I}$, is correlated with $c(k-N)$, while all samples $c(k), k \notin \mathcal{I} \cup \mathcal{I}'$, are independent.

The probability for all $2N+L$ samples of $c(k)$ to be observed simultaneously, given a certain value of θ, can be separated in the marginal probabilities for its samples to be observed, except for those samples $c(k), k \in \mathcal{I} \cup \mathcal{I}'$, which are pairwise correlated. Denote the joint probability density function for $c(k)$ and $c(k-N)$, $k \in \mathcal{I}$, by $p_1(\cdot)$, and the probability density function for $c(k), k \notin \mathcal{I} \cup \mathcal{I}'$, by $p_2(\cdot)$. Then, the log-likelihood function of θ given $c(k)$ becomes

$$\Lambda_{\mathrm{c}}(\theta) = \log p_\theta(c) = \tag{7}$$
$$\log\left\{\prod_{k\in\mathcal{I}} p_1\left(c(k), c(k-N)\right) \cdot \prod_{k\notin\mathcal{I}\cup\mathcal{I}'} p_2\left(c(k)\right)\right\}.$$

The ML estimator of θ given $c(k)$, $\hat{\theta}_c$, maximizes this function with respect to θ. For $k \notin \mathcal{I} \cup \mathcal{I}'$, $p_2(c(k)) = \frac{1}{4}$, since $r(k)$ is a zero-mean complex Gaussian process with independent real and imaginary parts. Hence, the second product in the maximization of (7) is a constant, which can be omitted. The ML estimate $\hat{\theta}_c$ becomes

$$\begin{aligned} \hat{\theta}_{\mathrm{c}} &= \arg\max_\theta \Lambda_{\mathrm{c}}(\theta) \\ &= \arg\max_\theta \sum_{k\in\mathcal{I}} \log p_1(c(k), c(k-N)) \\ &= \arg\max_\theta \sum_{k=\theta-L+1}^{\theta} \log p_1(c(k), c(k-N)) \\ &= \arg\max_\theta (g * h)(\theta), \end{aligned} \tag{8}$$

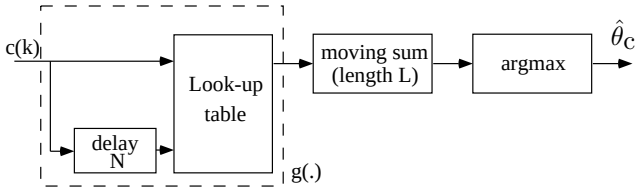

Fig. 4: Look-up table implementation of the ML estimator.

where

$$g(k) = \log p_1(c(k), c(k-N)), \tag{9}$$

$$h(k) = \begin{cases} 1, & 0 \le k < L-1, \\ 0, & \text{otherwise}, \end{cases} \tag{10}$$

and $*$ denotes convolution. To obtain the log-likelihood function we thus feed the sequence $c(k)$ through a nonlinearity $g(\cdot)$ and process the resulting sequence by means of a moving sum of length L, see Fig. 4. The ML estimation of θ selects the peaks of this function.

Fig. 4 suggests that the OFDM signal can be processed continuously. The sequence out of the moving sum is a concatenation of log-likelihood functions $\Lambda_C(\theta)$ for consecutive OFDM frames. In Fig. 5 such a sequence is shown.

In the appendix, the ML estimator based on $c(k)$ is determined by calculating the probability density $p_1(\cdot)$. Moreover, it is shown that taking the real part of the correlation between $c(k)$ and $c(k-N)$, instead of applying the non-linearity $g(k)$ yields an equivalent and attractive structure for the ML estimator, as illustrated in Figure 6. The estimate $\hat{\theta}_C$ feeds a *phase-locked loop* (PLL) in order to generate a frame clock.

C. Averaging the Log-Likelihood Function

In most applications the arrival time θ is approximately constant over several, say M, received frames. This essentially means that instead of just one frame $r(k)$, M frames are observed simultaneously containing information about the unknown θ. Generalizing the discussion preceding (7),

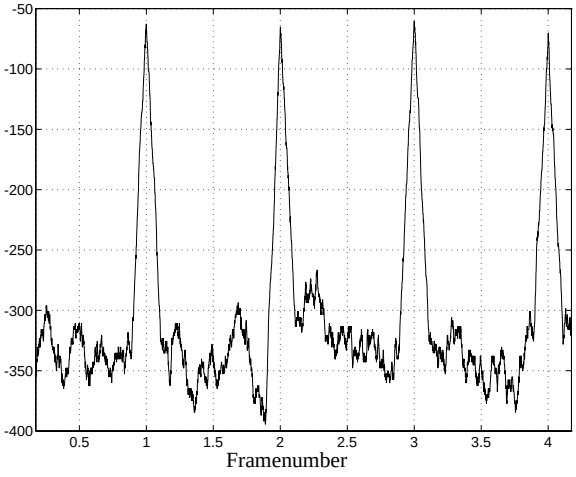

Fig. 5: Concatenated log-likelihood functions whose peaks generate estimates of θ. SNR=15 dB.

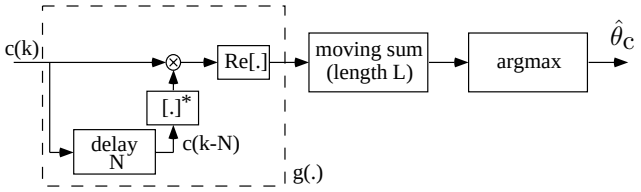

Fig. 6: Equivalent implementation of the ML estimator.

it can be shown that the log-likelihood function for θ given $c_i(k), i=1,\ldots,M$ becomes

$$\Lambda_a(\theta) \sim \sum_{i=1}^{M} \Lambda_C^i(\theta) \tag{11}$$

where $\Lambda_C^i(\theta)$ represents the log-likelihood function (7) of θ given frame $c_i(k)$. The ML estimate $\hat{\theta}_a$ given $c_i(k), i=1,\ldots,M$, is the argument maximizing (11).

IV. Simulations

We have performed Monte Carlo simulations to evaluate the performances of the suggested synchronization algorithms. First, the estimator performance for the AWGN channel is presented. Furthermore, two possible channel environments for OFDM, static and fading, are simulated. These environments both suffer from time dispersion, which makes the definition of the arrival time θ a delicate matter. In some sense, this arrival time and the influence of the channel on the data are interchangeable. In the following we will define the arrival time θ as the center of energy of the channel impulse response. We evaluate the performance of the estimator using the variance of the estimation error $E\{(\hat{\theta}-\theta)^2\}$.

Moreover, fading radio channels introduce a time-variant arrival time. This arrival time varies depending on the relative Doppler. This readily limits the usefulness of the averaging estimator. We present simulations of a slowly fading radio channel, allowing for moderate averaging.

A. AWGN Channel

An OFDM system consisting of 1024 subcarriers and a guardspace of 128 samples, *i.e.*, 1/8 of the frame length is considered. White, complex Gaussian noise is added and the error variance as a function of SNR is estimated. For each SNR value, 10,000 frames are simulated. Estimation error variance curves for the estimators $\hat{\theta}_c$ and $\hat{\theta}_a$, *i.e.*, the arguments maximizing (7) and (11), respectively, are compared to the ML estimator $\hat{\theta}_r$ that works on the unquantized OFDM-signal (2).

The simulations indicate that the estimators are approximately unbiased and the error variances $E\{(\hat{\theta}-\theta)^2\}$ are shown in Fig. 7. For practical channel environments, the assumption of infinite bandwidth is not realistic. The curves in Fig. 7 illustrate the performance of the derived estimators under ideal conditions. Notice the relative performances of the estimators. The estimator performance

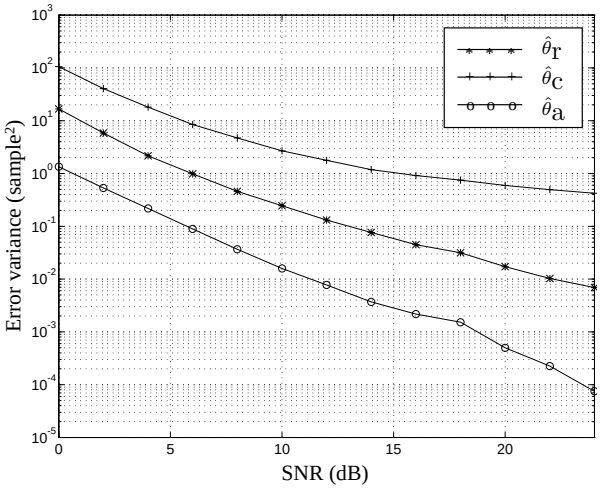

Fig. 7: Error variance for AWGN channel of three estimators: The ML estimator, $\hat{\theta}_r$, based on $r(k)$; the ML estimator, $\hat{\theta}_c$, based on the quantized data $c(k)$; and the averaging estimator, $\hat{\theta}_a$.

is degraded by regarding only the sign bits in the received signal $r(k)$. However, by averaging over only 8 consecutive frames before peak detection, the estimator performance is improved by a factor that is significantly larger than 64 (the improvement of averaging the estimates after the peak detection).

B. Twisted Pair Channel

A broadband OFDM system for HDSL with the following specifications is simulated. The impulse response of the channel, which is normalized to have unit energy, is obtained from measurements by Telia Research AB on a 503 meter copper wire and has a duration of approximately 2 μs. The sample frequency is 12.5 MHz, and the guardspace has a length of 128 samples, *i.e.*, 10.24 μs. The system uses 1024 subcarriers. Noise with a power spectral density proportional to $f^{3/2}$ is added to simulate

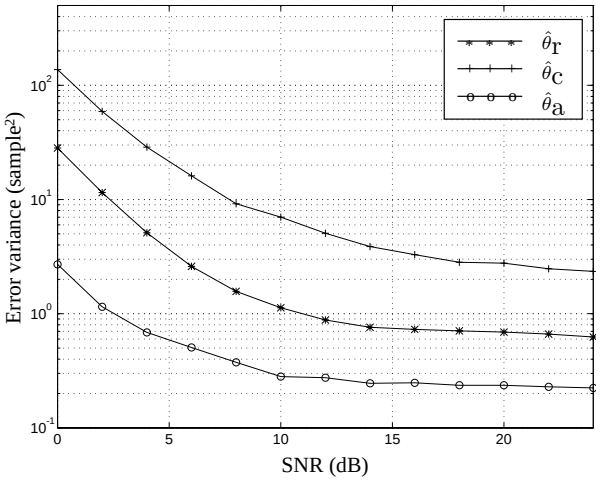

Fig. 8: Error variance for twisted pair channel of three estimators: The ML estimator, $\hat{\theta}_r$, based on $r(k)$; the ML estimator, $\hat{\theta}_c$, based on the quantized data $c(k)$; and the averaging estimator, $\hat{\theta}_a$.

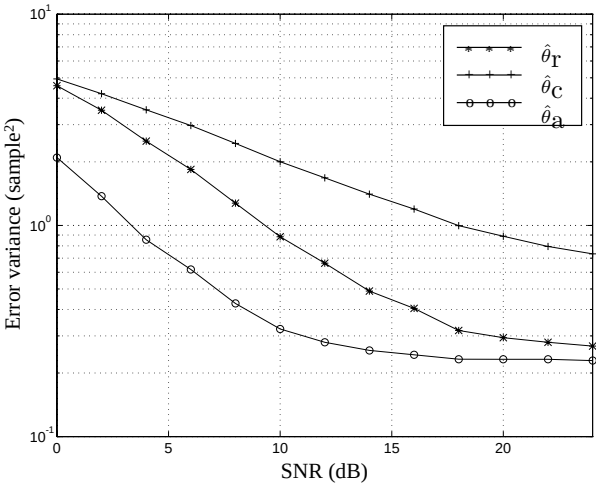

Fig. 9: Error variance for fading radio channel of three estimators: The ML estimator, $\hat{\theta}_r$, based on $r(k)$; the ML estimator, $\hat{\theta}_c$, based on the quantized data $c(k)$; and the averaging estimator, $\hat{\theta}_a$.

near-end crosstalk (NEXT) [5, 12]. The SNR in this case is defined as before, i.e. the quotient between signal and noise power at the receiver and again 10,000 frames are simulated for each SNR value.

The error variances are shown in Fig. 8. The estimators behave in approximately the same way as they do in a AWGN channel environment. The error variance, however, has increased, due to the channel impulse response of the copper wire, which bounds the error variance. Notice that the estimators are derived under the assumption that $c(k)$ are independent for $k \notin \mathcal{I} \cup \mathcal{I}'$. This assumption is violated as a consequence of the channel impulse response. However, the error variance of the estimator $\hat{\theta}_a$ is still small and may be used to feed a PLL.

C. Fading Radio Channel

Finally, we evaluate a slowly fading channel environment. A wireless system operating at 2 GHz with a bandwidth of 5 MHz is simulated. In these simulations, an OFDM frame consists of 64 subcarriers with an additional 5 sample guardspace. A fading environment with additive white Gaussian noise and large-room characteristics is chosen: the channel impulse response has a maximum length of 0.35 μs [13], corresponding to 2 samples. The channel impulse response is modelled to consist of two independent Rayleigh-fading taps with equal average power. The mobile is assumed to be moving at a maximum speed of 5 km/h resulting in a maximum Doppler frequency of 10 Hz. This Doppler frequency is low enough to motivate the averaging of 8 frames in the synchronization algorithm, since the channel impulse response does not change significantly during this interval. In this simulation, 300,000 frames are used for each SNR value.

The same effects as in the copper wire experiments can be observed from Fig. 9, *i.e.*, the proportions of the error variances resemble each other, but the absolute values have increased. Again, the channel bounds the error vari-

ance and the curves level out at ca. 15 dB. An increase of SNR beyond this threshold does not improve the estimators significantly.

V. Conclusions

In this paper we have shown how the cyclic extension of OFDM frames can be used to generate a frame clock at the receiver. The ML estimator $\hat{\theta}_{\mathrm{r}}$, based on the received data, though optimal, may not be appropriate for use in practical systems, due to its complexity. The ML estimation based on only the sign bits of the data is given for the AWGN channel model and an averaging over several OFDM frames is proposed. Simulations suggest that this averaging significantly improves synchronization performance. For practical systems on copper wires and slowly fading channels the error variance of $\hat{\theta}_{\mathrm{c}}$ is significantly improved. It can be used to feed a PLL, generating the system frame clock.

Appendix

Notice first that

$$c(k) = Q[r(k)] = a_l \Leftrightarrow r(k) \in \mathcal{Q}_l \tag{12}$$

where $\mathcal{Q}_l, l = 0, 1, 2, 3$ are the quadrants of the complex plane as depicted in Fig. 3. Since the real and imaginary part of $r(k)$ are independent, we can write the probability

$$\Pr(r(k)\in\mathcal{Q}_l) = \Pr(\mathrm{Re}\,\{r(k)\}\in\mathcal{H}_l)\Pr(\mathrm{Im}\,\{r(k)\}\in\mathcal{H}'_l) \tag{13}$$

(see Fig. 3), where $\mathcal{H}_l$ and $\mathcal{H}'_l$ are the half-planes

$$\mathcal{H}_l = \begin{cases} \mathbb{R}^+, & l = 0, 3 \\ \mathbb{R}^-, & l = 1, 2 \end{cases}, \quad \mathcal{H}'_l = \begin{cases} \mathbb{R}^+, & l = 0, 1 \\ \mathbb{R}^-, & l = 2, 3 \end{cases}. \tag{14}$$

The joint probability $p_1(\cdot)$ in (7) can be written as

$$\begin{aligned} &\Pr\left(c(k) = a_l, c(k-N) = a_n\right) = \\ &\quad \Pr\left(r(k)\in\mathcal{Q}_l, r(k-N)\in\mathcal{Q}_n\right) = \\ &\qquad \Pr\left(\mathrm{Re}\,\{r(k)\}\in\mathcal{H}_l, \mathrm{Re}\,\{r(k-N)\}\in\mathcal{H}_n\right)\times \\ &\qquad\quad \Pr\left(\mathrm{Im}\,\{r(k)\}\in\mathcal{H}'_l, \mathrm{Im}\,\{r(k-N)\}\in\mathcal{H}'_n\right). \end{aligned} \tag{15}$$

By applying the symmetry expressions for two real, zero-mean, jointly Gaussian variables x and y with correlation coefficient ρ, [14, pp. 137-138],

$$\begin{aligned} P^+ &\triangleq \Pr((x,y)\in\mathbb{R}^+\times\mathbb{R}^+) = \Pr((x,y)\in\mathbb{R}^-\times\mathbb{R}^-) \\ P^- &\triangleq \Pr((x,y)\in\mathbb{R}^-\times\mathbb{R}^+) = \Pr((x,y)\in\mathbb{R}^+\times\mathbb{R}^-), \end{aligned} \tag{16}$$

the look-up table in Fig. 4 becomes

$c(k-N)$	a_0	a_1	a_2	a_3
$c(k)$				
a_0	$\log P^+P^+$	$\log P^-P^+$	$\log P^-P^-$	$\log P^+P^-$
a_1	$\log P^+P^-$	$\log P^+P^+$	$\log P^-P^+$	$\log P^-P^-$
a_2	$\log P^-P^-$	$\log P^+P^-$	$\log P^+P^+$	$\log P^-P^+$
a_3	$\log P^-P^+$	$\log P^-P^-$	$\log P^+P^-$	$\log P^+P^+$

The ML estimate (8) that uses this look-up table is not affected by an affine scaling $f(x) = ax+b, (a>0)$ of the values in the table, since it is a convex mapping. If we choose

$$f(x) = \frac{x - \log P^+P^-}{\log P^+P^+ - \log P^+P^-} \tag{17}$$

the non-linearity $f[g(l,n)]$ becomes

$c(k-N)$	a_0	a_1	a_2	a_3
$c(k)$				
a_0	1	0	−1	0
a_1	0	1	0	−1
a_2	−1	0	1	0
a_3	0	−1	0	1

Since

$$\mathrm{Entry}(a_n, a_l) = \frac{1}{2}\mathrm{Re}\{a_n a_l^*\}, \tag{18}$$

the look-up table may be implemented by taking the real part of $c(k)c^*(k-N)$.

References

[1] J.A.C. Bingham, "Multicarrier modulation for data transmission: an idea whose time has come", *IEEE Communications Magazine*, Vol. 28, no. 5, pp. 5–14, May 1990.

[2] M. Alard and R. Lassalle, "Principles of modulation and channel coding for digital broadcasting for mobile receivers", *EBU Review*, no. 224, pp. 3–25, August 1987.

[3] B. Marti et al.,"European activities on digital television broadcasting—from company to cooperative projects", *EBU Technical Review*, no. 256, pp. 20–29, 1993.

[4] L.J. Cimini, Jr.,"Analysis and Simulation of a Digital Mobile Channel using Orthogonal Frequency Division Multiplexing", *IEEE Trans. Comm.*, Vol. COM–33, no. 7, pp. 665–675, July 1985.

[5] P.S. Chow, J.C. Tu, and J.M. Cioffi, "Performance evaluation of a Multichannel Transceiver System for ADSL and VHDSL Services", *IEEE J. Sel. Areas Comm.*,Vol. 9, no. 6, pp. 909–919, August 1991.

[6] K. Sistanizadeh, P.S. Chow and J.M. Cioffi, "Multi-Tone Transmission for Asymmetric Digital Subscriber Lines (ADSL)", *Proc. Intern. Conf. Comm.*, ICC '93, pp. 756–760, May 1993.

[7] W.D. Warner and C. Leung, "OFDM/FM Frame Synchronization for Mobile Radio Data Communication", *IEEE Trans. Veh. Techn.*, Vol. 42, no. 3, pp. 302–313, August 1993.

[8] P.J. Tourtier, R. Monnier and P. Lopez, "Multicarrier modem for HDTV terrestrial broadcasting", *Signal Processing: Image Communication*, Vol. 5, no. 5-6, pp. 379–403, December 1993.

[9] F. Daffara and O. Adami, "A new frequency detector for orthogonal multicarrier transmission techniques", In *Proc. VTC–95*, pp. 804–809, July1995.

[10] R. Gross and D. Veeneman, "Clipping Distortion in DMT ADSL Systems", *Electron. Lett.*, Vol. 29, no. 24, pp. 2080–2081, November 1993.

[11] M. Sandell, J.J. van de Beek, M. Isaksson, P.O. Börjesson, "Maximum Likelihood Synchronization in OFDM systems", To appear as a Research Report, Div. of Signal Processing, Luleå University, Sweden.

[12] J.-J. Werner, "The HDSL environment", *IEEE J. Sel. Areas Comm.*, Vol. SAC-9, no. 6, pp. 785–800, August 1991.

[13] U. Dersch and E. Zollinger, "Propagation Mechanism in Microcell and Indoor Environments", *Proc. 4th Intern. Symp. on Personal, Indoor and Mobile Radio Comm.*, PIMRC '93, Yokohama, Japan, pp. 191, September 1993.

[14] A. Papoulis, *Probability, Random Variables, and Stochastic Processes*, 2nd edition, McGraw-Hill, Inc., 1984